JOURNAL OF VIROLOGY, July 2005, p. 8142–8148 Vol. 79, No. 13
0022-538X/05/$08.00+0 doi:10.1128/JVI.79.13.8142–8148.2005

Preliminary Physical Mapping of RNA-RNA Linkages in the Genomic RNA of Moloney Murine Leukemia Virus

Catherine S. Hibbert and Alan Rein*

HIV Drug Resistance Program, National Cancer Institute—Frederick, Frederick, Maryland 21702-1201

Received 7 December 2004/Accepted 16 March 2005

Retrovirus particles contain two copies of their genomic RNA, held together in a dimer by linkages which presumably consist of a limited number of base pairs. In an effort to localize these linkages, we digested deproteinized RNA from Moloney murine leukemia virus (MLV) particles with RNase H in the presence of oligodeoxynucleotides complementary to specific sites in viral RNA. The cleaved RNAs were then characterized by nondenaturing gel electrophoresis. We found that fragments composed of nucleotides 1 to 754 were dimeric, with a linkage as thermostable as that between dimers of intact genomic RNA. In contrast, there was no stable linkage between fragments consisting of nucleotides 755 to 8332. Thus, the most stable linkage between monomers is on the 5′ side of nucleotide 754. This conclusion is in agreement with earlier electron microscopic analyses of partially denatured viral RNAs and with our study (C. S. Hibbert, J. Mirro, and A. Rein, J. Virol. 78:10927–10938, 2004) of encapsidated nonviral mRNAs containing inserts of viral sequence. We obtained similar results with RNAs from immature MLV particles, in which the dimeric linkage is different from that in mature particles and has not previously been localized. The 5′ and 3′ fragments of cleaved RNA are all held together by thermolabile linkages, indicating the presence of tethering interactions between bases 5′ and bases 3′ of the cleavage site. When RNAs from mature particles were cleaved at nucleotide 1201, we detected tethering interactions spanning the cleavage site which are intramonomeric and are as strong as the most stable linkage between the monomers.

In all normal retrovirus particles, the genomic RNA is in dimeric form (3). The dimer consists of two identical, positive-strand monomers. The linkage between them presumably consists of a limited number of base pairs. After the assembled virion is released from the cell, the viral protease (PR) cleaves the viral proteins into a series of smaller proteins (29); these cleavages, collectively resulting in the maturation of the particle, are required for the infectivity of the particle. Maturation of the virus also entails a change in the conformation of the dimeric RNA in the particle, frequently resulting in a more stable dimeric linkage than that present in immature virions (8, 9, 27). The change in conformation of the RNA, termed maturation of the dimer, is presumably due to the action of the nucleocapsid (NC) protein on the RNA; this protein is known to possess nucleic acid chaperone activity (the ability to catalyze the conformational rearrangement of nucleic acids into the structure with the maximum number of base pairs) and is tightly associated with the genomic RNA in the mature virion (6, 7, 16, 21, 26).

The location and structure of the linkage between the two monomers are not known with precision. Electron micrographs of partially denatured RNA extracted from mature retrovirus particles show that the locus of the most stable linkage is near, but not at, the 5′ end of the genome (1, 2, 13, 17). This region has therefore been termed the dimer linkage site (DLS). However, there is no information in the literature on the site of the linkage in immature dimers.

In recent years, it has been found that transcripts of the 5′ region of retroviral genomes can dimerize spontaneously in vitro under conditions of high ionic strength (4, 5, 20, 23). Apparently, this region of the genome always contains a stem-loop with a palindromic four- or six-base sequence in the loop. This motif is called the kissing loop (3). One obvious possible mechanism for dimer formation would be base pairing between the loops of two monomers, and convincing evidence has been obtained that this occurs during dimerization of transcripts in vitro. Further, an alternative dimeric conformation can also be envisioned in which the bases comprising the stems in the kissing-loop structure would come apart and form an extended dimer, with bases in both the stems and the loops paired intermolecularly. Thus, sequences present in retroviral DLS regions suggest a model not only for the structure of the dimer but even for the existence of two forms of dimer, one with a more stable linkage than the other. Indeed, experimental systems have been devised demonstrating that the transcripts can form two alternative species of dimer, and the human immunodeficiency virus type 1 (HIV-1) NC protein has been shown capable of converting the more labile species into the more stable species (7, 16, 22). However, it seems unlikely that the kissing-loop structure would give rise to dimers with the degree of thermostability found in retroviral genomic RNA.

Transcripts offer convenient model systems for experimental analysis and have proven to be a fruitful source of new concepts about viral RNAs. Ultimately, however, the validity of these concepts can only be tested by using authentic RNAs obtained from virus particles. In the present work, we have used a physical approach for mapping the locations of linkages present in immature and mature dimeric RNAs isolated from Moloney murine leukemia virus (MLV) particles. The results indicate that the most stable or primary linkage in immature

* Corresponding author. Mailing address: National Cancer Institute—Frederick, P.O. Box B, Frederick, MD 21702-1201. Phone: (301) 846-1361. Fax: (301) 846-7146. E-mail: rein@ncifcrf.gov.

dimers is, like that in mature dimers, near the 5′ end of the RNA. They also demonstrate the presence of additional intra- and intermolecular linkages in these RNAs.

MATERIALS AND METHODS

Cells and viruses. All virus preparations used in this work were produced by transient transfection of 293T cells with the wild-type MLV plasmid pRR88 or its PR^- derivative, containing a D32L mutation at the active site of PR (10).

RNA analysis. Methods for virus isolation, RNA preparation, and nondenaturing Northern blot analysis were described previously (9, 10). Dissociation of dimeric viral RNAs was monitored by nondenaturing Northern blotting following incubation of the RNA for 8 min at each incubation temperature in R buffer (50 mM NaCl, 10 mM Tris [pH 7.5], 1 mM EDTA, 1% sodium dodecyl sulfate [SDS]). Standard (denaturing) Northern blot assays were performed as previously described (24). The majority of experiments described here used a riboprobe complementary to MLV nucleotides (nt) 215 to 739 (10); the 3′ probe was a riboprobe complementary to nt 7830 to 8196.

RNase H digestion. When viral RNA was to be digested with RNase H, it was first deproteinized by proteinase K digestion in SDS and then extracted with phenol-chloroform, followed by ethanol precipitation in the presence of 0.3 M sodium acetate (pH 5.2) with 0.02% linear acrylamide. The pellet was resuspended in 100 μl R buffer lacking SDS. Ten microliters RNase-free DNase (Invitrogen) was added, and the RNA was incubated for 15 min at 25°C. The DNase was then removed with SDS and proteinase K digestion, and the RNA was re-extracted with phenol-chloroform-isoamyl alcohol (25:24:1) and reprecipitated with ethanol.

For RNase H digestion, the RNA pellet was washed twice with 70% ethanol and allowed to dry. It was then resuspended in RNase H buffer (50 mM KCl, 4 mM $MgCl_2$, 20 mM HEPES [pH 8.0], 1 mM freshly added dithiothreitol) using 95 μl buffer per 250 ml culture fluid. The RNA was then mixed with 5 μl of 100 μM oligodeoxynucleotide that had been heated in water to 90°C for 2 min. The oligonucleotide was allowed to anneal to the RNA for 5 min at 37°C. Five units of *Escherichia coli* RNase H (Roche Applied Science) was then added (maintaining the tube at 37°C), and the mixture was incubated at 37°C for 30 min. The reaction was terminated by addition of SDS to a concentration of 1.2% and was then deproteinized by sequential proteinase K digestion and phenol-chloroform-isoamyl alcohol extraction, followed by ethanol precipitation.

UV-psoralen cross-linking. Samples to be cross-linked were treated on ice with 20 μg/ml 4′-aminomethyl-4,5′,8-trimethylpsoralen (HRI Associates) in R buffer lacking SDS. They were then irradiated with 365-nm UV light at 1,700 $\mu W/cm^2$ for 10 min on ice. The control samples were also kept on ice until loading onto the gel.

RNA folding. Sequences were entered into Zuker's Mfold program (32) with no changes in the default settings. To look for possible complementarity within the viral RNA, a short stretch of viral sequence was entered into the program, followed by a string of 25 or more N (or A) residues and then by another short stretch of viral RNA. ΔG values were obtained from Mfold.

RESULTS

Site-specific cleavage of mature viral RNA. The goal of the present studies was to develop techniques for localizing RNA-RNA linkages in the dimeric RNA isolated from retroviral particles. The basic strategy in these studies was to cleave the RNA at a predetermined site, using RNase H in the presence of an oligodeoxynucleotide complementary to the site. The resulting fragments were then analyzed by nondenaturing gel electrophoresis.

In the first experiments, RNA extracted from mature MLV particles was digested by RNase H with an oligonucleotide complementary to nt 754 to 783 of the viral RNA. This site on the RNA is within the coding region for MA, ~130 nt 3′ of the Gag initiation codon at nt 621 and ~400 to 500 nt 3′ of the ψ/DLS region of the genome. (Identical results have also been obtained using an oligonucleotide complementary to nt 754 to 773.) Control samples were incubated with RNase H but without oligonucleotide. The results of this experiment, using Northern analysis with a probe against the 5′ region of the genome, are shown in Fig. 1. It can be seen that the RNA was indeed cleaved, since the probe-reactive material in the sample that was digested in the presence of oligonucleotide and heated to 65°C before electrophoresis has a high mobility and is near the bottom of the gel (lane 2D). In contrast, in the control sample that was mock digested in the absence of oligonucleotide, it migrates very slowly in the unheated sample (lane 1), and its mobility is only moderately increased by heating (lane 2). The bands seen in lanes 1 and 2 are the dimeric and monomeric genomic RNAs, respectively. The digestion product in lane 2D has a mobility consistent with a size of ~754 nt, as expected; the shift of virtually all the RNA reactive with the probe into this small, discrete fragment demonstrates the effectiveness of the enzymatic cleavage.

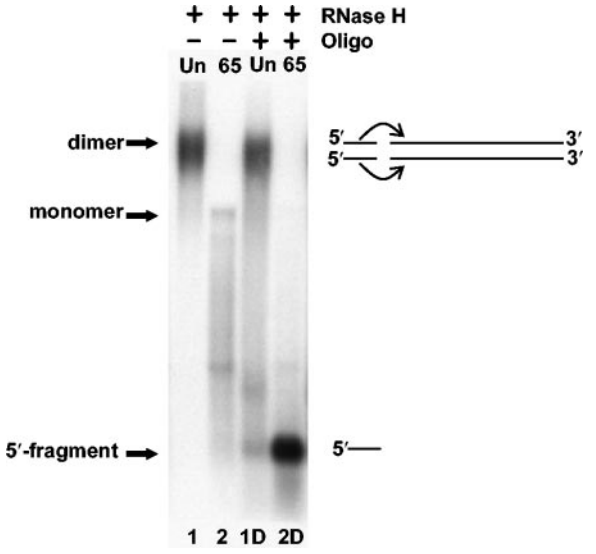

FIG. 1. RNase H cleavage of MLV RNA at nt 754. RNA from mature MLV virions was incubated with RNase H in the presence (lanes 1D and 2D) or absence (lanes 1 and 2) of an oligonucleotide (Oligo) complementary to MLV nt 754 to 783. It was then analyzed by nondenaturing Northern blotting before (lanes 1 and 1D; Un, unheated) or after (lanes 2 and 2D) heating to 65°C, using a probe complementary to nt 215 to 739. The presence of tethering interactions holding the fragments of the cleaved, unheated RNA together (lane 1D) is indicated in the illustration to the right.

We also analyzed the digested RNA without heating it before electrophoresis. As shown in lane 1D, this RNA had the same mobility as the uncleaved dimer (lane 1), despite the fact that it had been cleaved at nt 754 (lane 2D). These results show that the fragments of the digested RNA are held together until the RNA is heated. We conclude that native viral RNA contains thermolabile linkages connecting sequences on the 5′ side and those on the 3′ side of nt 754. We will refer to these linkages as tethering interactions. We cannot determine from these data whether these linkages are intermolecular, i.e., joining the 5′ end of one monomer to the 3′ fragment of the other, or intramolecular (or both).

It was of interest to determine the thermostability of these tethering interactions. We therefore repeated the digestion but heated the digested RNA stepwise before electrophoresis. As shown in Fig. 2A, when the RNA was heated to 50 or 55°C

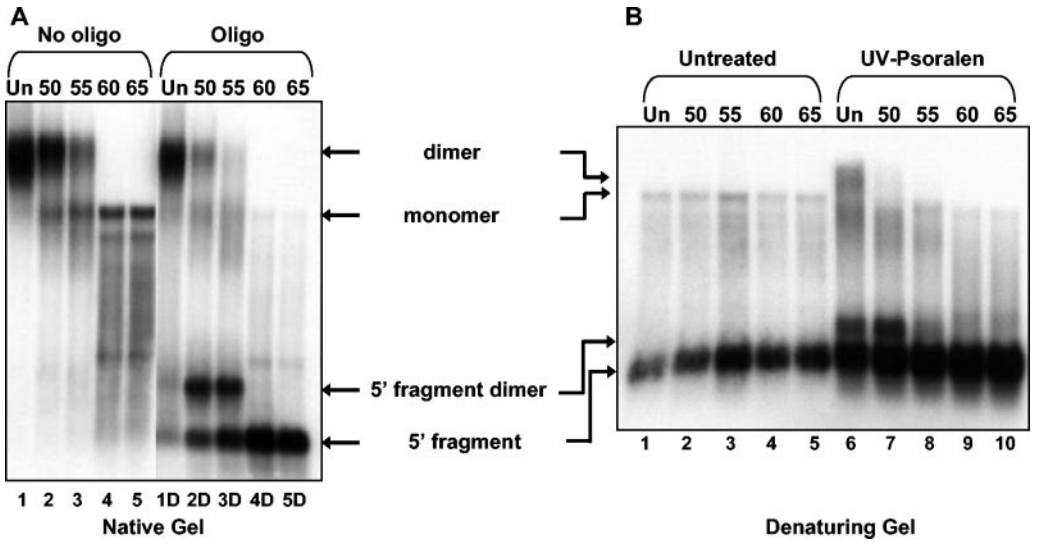

FIG. 2. Thermostability of RNA-RNA linkages in cleaved MLV RNA. (A) RNA from mature MLV virions was cleaved as described in the legend to Fig. 1 and incubated at different temperatures before analysis as described in the legend to Fig. 1. The temperatures are indicated at the top. Un, unheated sample. Results are shown for RNA incubated with RNase H in the absence (lanes 1 to 5) or presence (lanes 1D to 5D) of oligonucleotide (oligo). The RNA migrating as a dimer in lanes 1D and 2D has been cleaved by the RNase H but is still held together by thermolabile tethering interactions. (B) The samples shown in lanes 1D to 5D of panel A, in which the cleaved RNA had been incubated at different temperatures, were analyzed by denaturing Northern analysis without (lanes 1 to 5) or with (lanes 6 to 10) UV-psoralen cross-linking.

before electrophoresis, a new band appeared (lanes 2D and 3D). This band migrates much more rapidly than the full-length dimers and monomers seen when the oligonucleotide is omitted from the digestion (lanes 1 to 5) but more slowly than the fragment obtained when the digested RNA is heated to 65°C (lane 5D). Heating to 60° is sufficient to produce the latter fragment (lane 4D).

Our interpretation of these results is as follows. The tethering interaction holding the two digestion products together is broken by incubating the digest at 50°C. However, as shown in lanes 1 to 5, the most stable dimeric linkage between the genomic RNA monomers withstands heating to 55°C and is not broken until the RNA is incubated at 60°C. This linkage is evidently on the 5′ side of nt 754, since the digestion products consisting of nt 1 to 754 are held together in a 5′ fragment dimer (the new band in lanes 2D and 3D) until the RNA is heated to 60°C. (These data do not exclude the possibility that an equally stable dimeric linkage also exists 3′ to nt 754.)

Psoralens cause the chemical cross-linking of base-paired or closely associated RNA strands upon UV irradiation (for example, see references 28 and 30). To confirm the identities of the bands observed in Fig. 2A, we performed UV-psoralen cross-linking on aliquots of the digested samples that had been heated to different temperatures (shown in lanes 1D to 5D). The cross-linked RNAs, along with control aliquots that were not UV-psoralen treated, were then analyzed by electrophoresis under denaturing conditions, followed by hybridization with the 5′ probe as described above. Results of this experiment are shown in Fig. 2B. In the absence of the cross-linking treatment, virtually all of the RNA reacting with the probe was in the rapidly migrating fragment (lanes 1 to 5). A similar profile was observed with the samples that had been heated to 60 to 65°C before cross-linking (lanes 9 and 10). The same fragment was also present in lanes 6 to 8; in addition, however, the sample that was cross-linked without being heated after digestion (lane 6) showed some radioactivity in a high-molecular-weight band and also contained a prominent band migrating only slightly more slowly than the band present in lanes 1 to 5. The latter species was also seen in the samples heated to 50 or 55°C (lanes 7 and 8, respectively) (this species was considerably fainter in lane 8 than in lanes 6 and 7).

The UV-psoralen cross-linking results in Fig. 2B appear to be fully consistent with our interpretation of Fig. 2A. Three species were observed when the digested samples were analyzed by nondenaturing gel electrophoresis (Fig. 2A, lanes 1D to 5D): the tethered dimer, the 5′ fragment dimer, and the 5′ fragment. Each of these was also seen in the cross-linked samples; thus, even though the genomic RNA was quantitatively cleaved in the digestion, the 5′-end cleavage product was retained in complexes that could be covalently linked by UV-psoralen treatment, enabling them to survive the denaturing electrophoretic conditions used in Fig. 2B. These complexes were destroyed by exposure to 60°C.

Site-specific cleavage of immature viral RNA. We have previously reported (9) that the dimeric linkage in genomic RNA isolated from immature MLV particles, in which Gag has not been cleaved by the viral protease, is less stable than that in RNA from mature particles. There is no information now in the literature regarding the physical location of this linkage. We therefore analyzed the genomic RNA from PR^- MLV particles, using the same strategy as in Fig. 2A above. As shown in Fig. 3A, the dimeric RNAs in the mock-digested sample (incubated with RNase H in the absence of oligodeoxynucleotide) were partially dissociated to monomers by exposure to 50°C and completely dissociated at 55°C (lanes 2 to 3), in agreement with our earlier results (9). (Heating to 60°C also generates a band ~2 kb in size; we do not know the exact nature of this species.) Material reacting with the probe in the

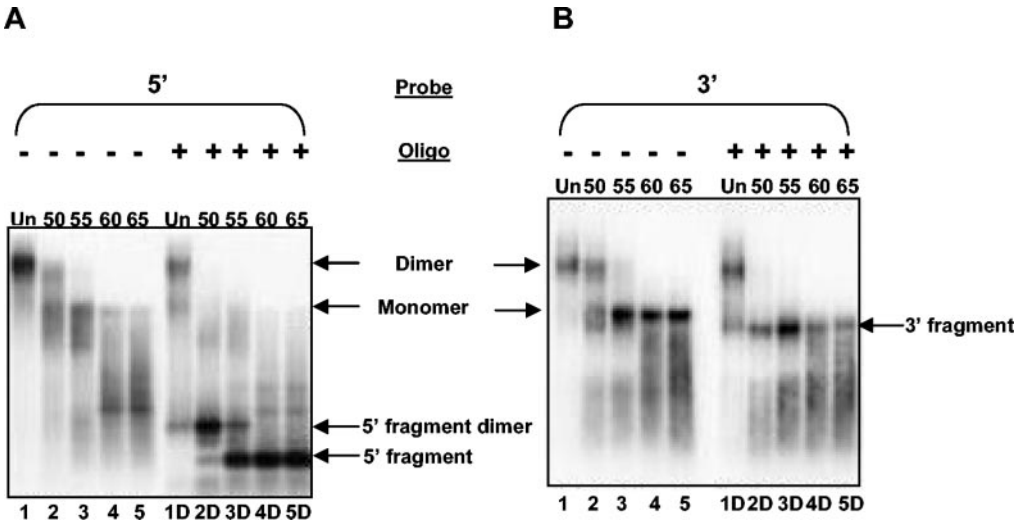

FIG. 3. RNA-RNA linkages in immature MLV RNA. (A) RNA from PR$^-$ MLV virions was analyzed exactly as in Fig. 2A. All samples were incubated with RNase H, but the RNA was not cleaved in the absence of oligonucleotide (oligo; lanes 1 to 5). (B) The membrane shown in panel A was stripped and then reprobed with radioactive RNA complementary to MLV nt 7830 to 8196. Un, unheated.

digested sample was distributed between a band corresponding in mobility to dimeric RNA, a faint band corresponding to monomeric RNA, and a rapidly migrating band with mobility suggesting a size of ~1.5 kb (lane 1D). When this sample was heated to 50°C before electrophoresis, virtually all of the reactive material was shifted into the 1.5-kb band (lane 2D). Higher temperatures in turn shifted the material into a still smaller species (lanes 3D to 5D).

The data in Fig. 3A are completely analogous to those obtained with mature dimeric RNA and shown in Fig. 2B; the only difference is that the dimeric linkage between the monomers of full-length (lanes 1 to 3) and 5′ fragments (lanes 1D to 3D) of the cleaved genomic RNA can be broken by incubation at 55°C, rather than 60°C. Thus, the results demonstrate that the linkage on the 5′ side of nt ~754 is as thermostable as the most stable linkage in the genomic dimers. In addition, they show that immature dimers, like mature dimers, contain a weak tethering linkage bridging the gap created at nt ~754 by the RNase H.

The above findings are consistent with the hypothesis that the most stable linkage between the monomers is at a single site, located on the 5′ side of nt 754. However, it is also conceivable that there are one or more additional linkages of equal stability at sites 3′ of nt 754. To test this possibility, we reprobed the membrane used in Fig. 3A with a probe complementary to nt 7830 to 8196. The results are shown in Fig. 3B. We found (lane 2D) that heating the digested RNA to 50°C generates a single species migrating only slightly more rapidly than monomeric RNA (the expected size of the 3′ fragment produced by cleavage at nt 754 is ~7.6 kb.) Thus, 50°C is evidently sufficient to disrupt all linkages between the monomers 3′ of nt 754. We have also obtained similar results with mature dimeric RNA (data not shown).

Specific cleavage at other sites. We also attempted to cleave viral RNA at other sites. In many cases, these experiments were unsuccessful; it seems likely that with many oligodeoxynucleotides, annealing to the RNA is quite inefficient because our protocol precludes the use of temperatures above 37°C in the hybridization reaction. However, two oligonucleotides producing near-quantitative cleavage of the RNA were identified. One of these, complementary to MLV nt 713 to 742, gave results quite similar to those described above. As shown in Fig. 4, lanes 1 to 6, stepwise heating of mature dimeric RNA that had been digested in the presence of this oligonucleotide gradually shifted the probe-reactive material from the mobility of full-length dimeric RNA to that of a dimer fragment. This shift was nearly complete at 52.5°C. Incubation at 55°C (lane 7) dissociated this dimer into monomeric fragments. This oligonucleotide also produced results similar to nt 754 with immature dimeric RNA (data not shown). These results indicate that the most stable linkage in dimeric RNA (i.e., the linkage that is only dissociated at 55°C) is located 5′ of nt 713 and also that there are tethering interactions between sequences on the 5′ side and those on the 3′ side of nt 713.

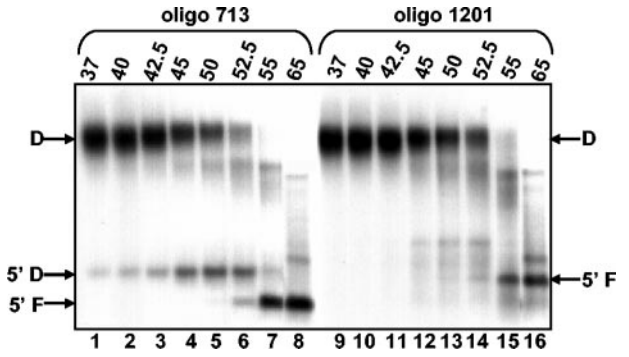

FIG. 4. Linkages in MLV RNA following cleavage at nt 713 or 1201. RNA from mature MLV virions was incubated with RNase H in the presence of oligonucleotides (oligo) complementary to MLV nt 713 to 742 (lanes 1 to 8) or 1201 to 1230 (lanes 9 to 16). They were then heated at the temperatures indicated at the top before analysis as in Fig. 1. D, dimer; 5′ D, dimer of 5′ fragment; 5′ F, monomer of 5′ fragment.

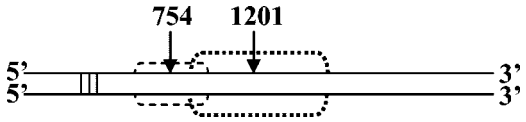

FIG. 5. Schematic depiction of linkages in MLV RNA. The figure shows that the most stable linkage between monomers in MLV dimeric RNA is on the 5′ side of nt 754 (shown as solid vertical lines). In addition, there are tethering linkages joining sequences on the 5′ side of nt 754 to sequences on the 3′ side; these are shown as dashed lines. These linkages, which are less thermostable than the most stable linkage, could be either intra- or intermonomeric, although they are depicted as intramonomeric. There are also bonds connecting sequences between nt 754 and nt 1201 with sequences to the 3′ side of nt 1201 (shown as dotted lines). These are as stable as the most stable linkage and are exclusively intramonomeric. Intervals are not drawn to scale.

When MLV RNA was digested with an oligonucleotide complementary to nt 1201 to 1230, the results were significantly different from those described above. In this case, there was no change in the mobility of the probe-reactive material up to a temperature of 52.5°C (Fig. 4, lanes 9 to 14). Upon incubation at 55°C, this material was abruptly converted into the ~1,201-base monomeric fragment (lane 15). The implications of these data are discussed below.

DISCUSSION

In the experiments described here, we have used site-specific cleavage to begin to localize the RNA-RNA linkages in the dimeric RNA present in MLV particles. The results led to two primary conclusions: first, the most stable linkage between the monomers of viral RNA is near the 5′ ends of the molecules; and second, these RNAs also contain other linkages, which we detected by the fact that the electrophoretic mobility of cleaved RNAs did not change until they were heated. We termed these additional linkages tethering interactions.

The localization of the most stable linkage near the 5′ end of the RNA is fully consistent with images of partially denatured viral RNA obtained by electron microscopy (1, 2, 11, 13, 17). It is also in agreement with our recent studies on nonviral RNAs containing limited MLV-derived sequences in their 3′ untranslated regions: we found that mRNAs with sequences from the 5′ end of viral RNA are not only encapsidated but are present

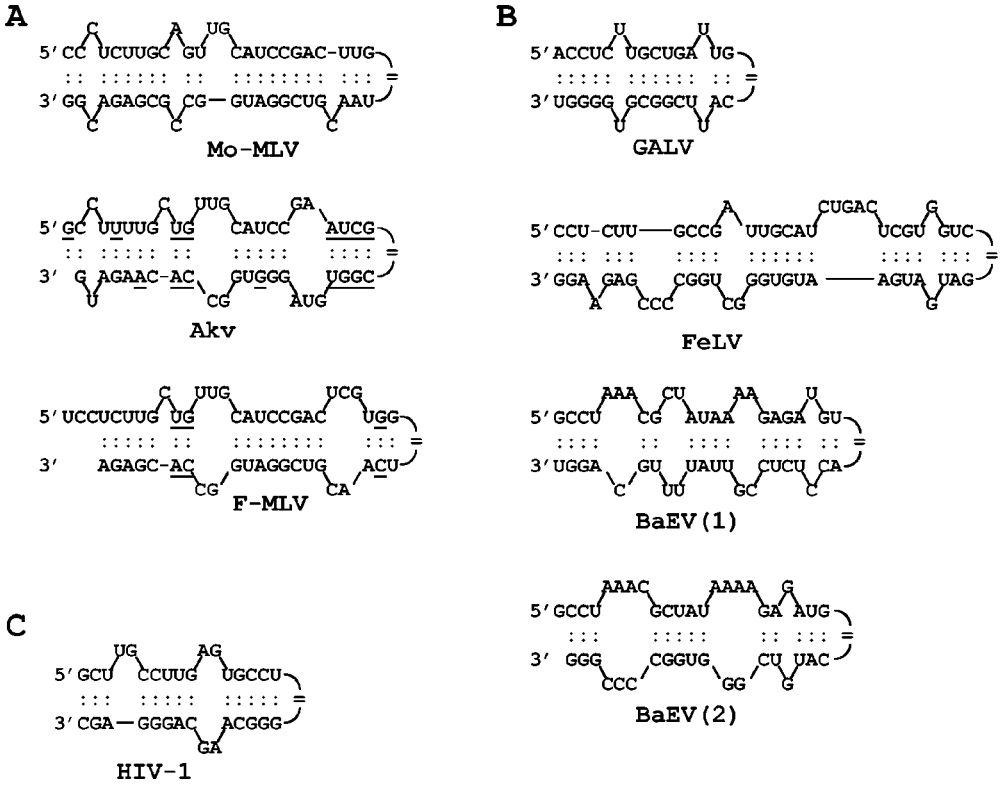

FIG. 6. Potential tethering interactions in retroviral genomes. The figure shows possible base pairings between segments of retroviral genomes. In each case, the first nucleotide shown is the nucleotide immediately following the AATAAA polyadenylation signal. (A) MLV RNAs: Moloney MLV (Mo-MLV; GenBank accession no. J02255), complementarity between nt 53 to 77 and nt 758 to 781; AKR MLV (Akv; accession no. J01998), complementarity between nt 53 to 77 and nt 776 to 798; Friend MLV (F-MLV; accession no. Z11128), complementarity between nt 53 to 80 and nt 755 to 776. Sequence changes in AKR MLV and Friend MLV relative to Moloney MLV which preserve base pairing are underlined. (B) Other gammaretroviral RNAs: gibbon ape leukemia virus (GALV; accession no. M26927), complementarity between nt 53 to 67 and nt 764 to 778; feline leukemia virus (FeLV; accession no. M18247), complementarity between nt 393 to 422 and nt 1037 to 1066; baboon endogenous virus (BaEV; accession no. d10032) 1, complementarity between nt 383 to 406 and nt 1154 to 1175; 2, complementarity between nt 383 to 406 and nt 1123 to 1141. Nucleotides 1123 to 1141 (structure 2) are in the same position in the MA coding region as shown for the other viruses in panels A and B, but structure 1 is somewhat more stable than structure 2. (C) HIV-1 Mal RNA (accession no. X04415), complementarity between nt 77 to 93 and nt 456 to 470.

in virions as dimers with the same thermostability as that of dimeric genomic RNA (10).

Our present studies also represent the first data on the localization of the linkage between monomers in immature dimeric RNAs (i.e., the dimers present in immature virus particles). We found that this linkage is also near the 5′ end of viral RNA. This conclusion is in harmony with our previous findings on nonviral mRNAs containing viral inserts (10). The mapping data are fully consonant with the simple hypothesis that the most stable linkage in immature dimers is a kissing complex at the dimer initiation site (DIS) and that the appearance of free NC upon virion maturation converts this complex to an extended dimer, in which the stems, as well as the loops, of the DIS stem-loop are engaged in intermolecular base pairing. However, the thermostability of the dimers suggests that they are likely stabilized by additional interactions in or near the DIS; results in our studies on nonviral RNAs (10) also indicated that the nature of the linkages is considerably more complex than this simple idea.

The second basic finding presented here is the existence of tethering interactions within viral RNAs. Since the earliest investigations of retroviral RNAs (15), it has frequently been observed that dimeric RNAs appear intact even when they are composed of stochastically fragmented monomers (18). This observation shows that viral RNAs contain linkages other than the primary or most stable dimeric linkage but does not allow one to draw any inferences concerning the locations of these secondary linkages. In contrast to the random fragmentation characteristic of many viral RNA preparations, we have used RNase H to break all the monomers at the same position. Our results show that both immature and mature MLV RNAs contain bonds joining sequences on the 5′ side of nt 754 to those on the 3′ side of this position. These bonds could be either intra- or intermolecular; in other words, we cannot determine whether the 5′ fragment of one monomer is linked to the 3′ fragment of the same or the other monomer in the dimeric complex.

Somewhat different results were obtained with RNAs cleaved near nt 1201. In these experiments, the tethering interactions holding the dimeric complex together were only broken at 55°C (Fig. 4, lanes 9 to 16), the same temperature at which intact dimers are dissociated into monomers. As noted above, when the RNAs are cleaved at nt ~754, the 3′ fragments are not held together by stable bonds (Fig. 3B); therefore, the tethering linkages spanning nt 1201 must be intramolecular, joining the 5′ fragment of one monomer to the 3′ fragment of the same monomer. Our conclusions regarding the location and stability of linkages in viral RNA are diagrammed in Fig. 5.

What are the actual locations of these tethering interactions? There are obviously many possibilities for base pairing within the dimers of 8.3-kb viral RNAs. We searched for possible pairings within the MLV RNA sequence. It is interesting to note the complementarity between sequences at nt 53 to 77 and those at nt 758 to 781. As shown in Fig. 6A, folding the RNA could, in theory, lead to a structure with 11 G-C base pairs and 10 other base pairs; calculations in Mfold indicate that the ΔG associated with this structure is −20.5 kcal/mol. Perhaps this structure (or a portion of it) is responsible for the tethering interaction we detected in viral RNAs cleaved at nt ~754; it should be noted that we do not know the precise site of cleavage with oligonucleotides complementary to nt 754 to 773 or −783, as used in Fig. 1 to 3. This fold would pair sequences immediately 3′ of the poly(A) signal in the R region with sequences in the MA coding region of *gag*. To obtain some sense of the conservation of such a structure, we also examined the sequences of a number of other murine leukemia virus isolates; in fact, all of them could be folded into similar structures, in each case with the 5′ end of the structure immediately following the AAUAAA polyadenylation signal. Two of these other putative murine leukemia virus structures are shown in Fig. 6A, with mutations preserving base pairing highlighted. We also found equivalent hypothetical structures in the genomes of other gammaretroviruses, including gibbon ape leukemia virus, feline leukemia virus, and baboon endogenous virus, despite the fact that that these sequences are considerably more divergent than those of different murine leukemia virus isolates. These hypothetical structures are shown in Fig. 6B. (Two possible structures are shown in the case of baboon endogenous virus.) Finally, recent studies (19) have demonstrated the existence of a pseudoknot in HIV-1 RNA transcripts, in which nt 77 to 83, immediately 3′ of the poly(A) signal, pair with nt 457 to 463, in the MA coding sequence. This structure appears quite analogous to the hypothetical folds shown in Fig. 6A and B. Examination of the sequence of HIV-1 RNA actually suggests the possibility of a more extensively base-paired structure at this site, as shown in Fig. 6C.

Long-range interactions have previously been described in several cellular and viral RNAs; several of these have regulatory effects on RNA function (12, 14, 25, 31). In the case of retroviruses, there are many possible functional roles for such a structure. Thus, it might well function in compacting the genomic RNA, facilitating its confinement in the interior of the virion. By affecting the three-dimensional structure of the leader region, it might contribute to the discrimination between full-length RNAs, which are substrates for encapsidation and contain the MA coding region, and spliced RNAs, which are not. It might also interfere with the recognition of the poly(A) signal in the 5′ region of the viral RNA, facilitating the synthesis of full-length RNA by RNA polymerase II. (This function would presumably be required in retroviruses in which the poly(A) signal is within R; these viruses include the gammaretroviruses like MLV and lentiviruses such as HIV-1. In contrast, the poly(A) signal in alpha- and deltaretroviruses is in U3 and thus is not present in the 5′ region of genomic RNA.) Another role might be to inhibit translation, helping to remove some genomic RNA molecules from the mRNA pool so that they are available for encapsidation. Further analysis will obviously be needed to identify the sites of tethering interactions in viral RNA and to elucidate their functional significance.

ACKNOWLEDGMENT

We thank Jane Mirro for consistently superb technical assistance.

REFERENCES

1. **Bender, W., Y. H. Chien, S. Chattopadhyay, P. K. Vogt, M. B. Gardner, and N. Davidson.** 1978. High-molecular-weight RNAs of AKR, NZB, and wild mouse viruses and avian reticuloendotheliosis virus all have similar dimer structures. J. Virol. **25:**888–896.
2. **Bender, W., and N. Davidson.** 1976. Mapping of poly(A) sequences in the electron microscope reveals unusual structure of type C oncornavirus RNA molecules. Cell **7:**595–607.

3. **Berkowitz, R., J. Fisher, and S. P. Goff.** 1996. RNA packaging. Curr. Top. Microbiol. Immunol. **214:**177–218.
4. **Bieth, E., C. Gabus, and J. L. Darlix.** 1990. A study of the dimer formation of Rous sarcoma virus RNA and of its effect on viral protein synthesis in vitro. Nucleic Acids Res. **18:**119–127.
5. **Darlix, J. L., C. Gabus, M. T. Nugeyre, F. Clavel, and F. Barre-Sinoussi.** 1990. cis elements and trans-acting factors involved in the RNA dimerization of the human immunodeficiency virus HIV-1. J. Mol. Biol. **216:**689–699.
6. **Darlix, J. L., M. Lapadat-Tapolsky, H. de Rocquigny, and B. P. Roques.** 1995. First glimpses at structure-function relationships of the nucleocapsid protein of retroviruses. J. Mol. Biol. **254:**523–537.
7. **Feng, Y. X., T. D. Copeland, L. E. Henderson, R. J. Gorelick, W. J. Bosche, J. G. Levin, and A. Rein.** 1996. HIV-1 nucleocapsid protein induces "maturation" of dimeric retroviral RNA in vitro. Proc. Natl. Acad. Sci. USA **93:**7577–7581.
8. **Fu, W., R. J. Gorelick, and A. Rein.** 1994. Characterization of human immunodeficiency virus type 1 dimeric RNA from wild-type and protease-defective virions. J. Virol. **68:**5013–5018.
9. **Fu, W., and A. Rein.** 1993. Maturation of dimeric viral RNA of Moloney murine leukemia virus. J. Virol. **67:**5443–5449.
10. **Hibbert, C. S., J. Mirro, and A. Rein.** 2004. mRNA molecules containing murine leukemia virus packaging signals are encapsidated as dimers. J. Virol. **78:**10927–10938.
11. **Hoglund, S., A. Ohagen, J. Goncalves, A. T. Panganiban, and D. Gabuzda.** 1997. Ultrastructure of HIV-1 genomic RNA. Virology **233:**271–279.
12. **Honda, M., R. Rijnbrand, G. Abell, D. Kim, and S. M. Lemon.** 1999. Natural variation in translational activities of the 5′ nontranslated RNAs of hepatitis C virus genotypes 1a and 1b: evidence for a long-range RNA-RNA interaction outside of the internal ribosomal entry site. J. Virol. **73:**4941–4951.
13. **Kung, H. J., S. Hu, W. Bender, J. M. Bailey, N. Davidson, M. O. Nicolson, and R. M. McAllister.** 1976. RD-114, baboon, and woolly monkey viral RNA's compared in size and structure. Cell **7:**609–620.
14. **Lanchy, J. M., C. A. Rentz, J. D. Ivanovitch, and J. S. Lodmell.** 2003. Elements located upstream and downstream of the major splice donor site influence the ability of HIV-2 leader RNA to dimerize in vitro. Biochemistry **42:**2634–2642.
15. **Mangel, W. F., H. Delius, and P. H. Duesberg.** 1974. Structure and molecular weight of the 60-70S RNA and the 30-40S RNA of the Rous sarcoma virus. Proc. Natl. Acad. Sci. USA **71:**4541–4545.
16. **Muriaux, D., H. De Rocquigny, B. P. Roques, and J. Paoletti.** 1996. NCp7 activates HIV-1Lai RNA dimerization by converting a transient loop-loop complex into a stable dimer. J. Biol. Chem. **271:**33686–33692.
17. **Murti, K. G., M. Bondurant, and A. Tereba.** 1981. Secondary structural features in the 70S RNAs of Moloney murine leukemia and Rous sarcoma viruses as observed by electron microscopy. J. Virol. **37:**411–419.
18. **Ortiz-Conde, B. A., and S. H. Hughes.** 1999. Studies of the genomic RNA of leukosis viruses: implications for RNA dimerization. J. Virol. **73:**7165–7174.
19. **Paillart, J. C., E. Skripkin, B. Ehresmann, C. Ehresmann, and R. Marquet.** 2002. In vitro evidence for a long range pseudoknot in the 5′-untranslated and matrix coding regions of HIV-1 genomic RNA. J. Biol. Chem. **277:**5995–6004.
20. **Prats, A. C., C. Roy, P. A. Wang, M. Erard, V. Housset, C. Gabus, C. Paoletti, and J. L. Darlix.** 1990. *cis* elements and *trans*-acting factors involved in dimer formation of murine leukemia virus RNA. J. Virol. **64:**774–783.
21. **Rein, A., L. E. Henderson, and J. G. Levin.** 1998. Nucleic acid chaperone activity of retroviral nucleocapsid proteins: significance for viral replication. Trends Biochem. Sci. **23:**297–301.
22. **Rist, M. J., and J. P. Marino.** 2002. Mechanism of nucleocapsid protein catalyzed structural isomerization of the dimerization initiation site of HIV-1. Biochemistry **41:**14762–14770.
23. **Roy, C., N. Tounekti, M. Mougel, J. L. Darlix, C. Paoletti, C. Ehresmann, B. Ehresmann, and J. Paoletti.** 1990. An analytical study of the dimerization of in vitro generated RNA of Moloney murine leukemia virus MoMuLV. Nucleic Acids Res. **18:**7287–7292.
24. **Sambrook, J., and D. W. Russell.** 2001. Molecular cloning: a laboratory manual, 3rd ed. Cold Spring Harbor Laboratory Press, Cold Spring Harbor, N.Y.
25. **Scheper, W., D. Meinsma, P. E. Holthuizen, and J. S. Sussenbach.** 1995. Long-range RNA interaction of two sequence elements required for endonucleolytic cleavage of human insulin-like growth factor II mRNAs. Mol. Cell. Biol. **15:**235–245.
26. **Stewart, L., G. Schatz, and V. M. Vogt.** 1990. Properties of avian retrovirus particles defective in viral protease. J. Virol. **64:**5076–5092.
27. **Stoltzfus, C. M., and P. N. Snyder.** 1975. Structure of B77 sarcoma virus RNA: stabilization of RNA after packaging. J. Virol. **16:**1161–1170.
28. **Swanstrom, R., L. M. Hallick, J. Jackson, J. E. Hearst, and J. M. Bishop.** 1981. Interaction of psoralen derivatives with the RNA genome of Rous sarcoma virus. Virology **113:**613–622.
29. **Swanstrom, R., and J. W. Wills.** 1997. Synthesis, assembly, and processing of viral proteins, p. 263–334. *In* J. M. Coffin, S. H. Hughes, and H. E. Varmus (ed.), Retroviruses. Cold Spring Harbor Laboratory Press, Plainview, N.Y.
30. **Wollenzien, P., J. E. Hearst, P. Thammana, and C. R. Cantor.** 1979. Base-pairing between distant regions of the Escherichia coli 16S ribosomal RNA in solution. J. Mol. Biol. **135:**255–269.
31. **Zhang, G., V. Slowinski, and K. A. White.** 1999. Subgenomic mRNA regulation by a distal RNA element in a (+)-strand RNA virus. RNA **5:**550–561.
32. **Zuker, M.** 2003. Mfold web server for nucleic acid folding and hybridization prediction. Nucleic Acids Res. **31:**3406–3415.